High-Efficiency Solar Concentrator

F. L. Lansing and J. Dorman
DSN Engineering Section

A new type of solar concentrator is presented using liquid lenses and simple translational tracking mechanism. The concentrator achieves a 100:1 nominal concentration ratio and is compared in performance with a flat-plate collector having two sheets of glazing and non-selective coating. The results of the thermal analysis show that higher temperatures can be obtained with the concentrator than is possible with the non-concentrator flat-plate type. Furthermore, the thermal efficiency far exceeds that of the comparative flat-plate type for all operating conditions.

I. Introduction

One of the fundamental problems associated with the effort to replace conventional energy sources by solar energy is to achieve high-temperature collection at very low cost. High temperature is feasible if the solar energy is concentrated and delivered to a collecting medium such as a gas or liquid. The greater the energy concentration, the greater the temperature of the collecting medium and the more useful the energy collected for heating, airconditioning, and electric power generation. Unfortunately, low-cost flat-plate solar collectors cannot operate efficiently at temperatures above 100°C, and presently available higher temperature concentrators are very expensive (approximately 5 to 10 times the cost of flat-plate collectors).

This article describes a low-cost method of manufacturing a high-temperature solar concentrator. There are two main features of the design that are unique: (a) a liquid lens construction of optimum shape with 100:1 nominal concentration ratio, and (b) a translational rather than rotational tracking mechanism. There is a resemblance between the construction of this design to that of a simple, non-concentrating flat-plate solar collector having two sheets of glazing, and it is estimated that it will cost only approximately 25 percent more for the liquid lens construction.

II. Description

The main features of the solar concentrator are indicated in Fig. 1. The major elements of the device are the lens assembly, working medium tubes, and the tracking mechanism. The lens assembly forms a series of individual lenses arranged side by side and is fabricated from transparent plastic or glass, as illustrated in Fig. 2. The curvature of the upper and lower shells of the lens assembly is designed for minimum focal length and optimum concentration ratio. The space between shells is filled with liquid. The initial design used water as the filling medium

for its low cost. The refraction index of water (1.33) closely approximates that of glass (1.5) so that the lens optical transmissivity closely approximates that achieved by a solid lens manufactured from glass. It is foreseen that other transparent liquids or additives may enhance the performance of the concentrator for different applications. The lens assembly design also includes compensation for expansion and the contraction of the liquid filler in addition to means for filling, draining, and cleaning (not shown in figures). The outer shells of the lens assembly are inexpensive to manufacture and light in weight for easy shipment and site installation.

The working medium tubes can be made of copper, steel, or aluminum and are placed on a thermal insulation layer at the focal lines of the individual lenses. There is no fin or plate connection of the tubes as is normal with flat-plate solar collectors. The tube surface is coated with a mat black paint for maximum absorption. A nominal concentration ratio of 100:1 was demonstrated experimentally on the single lens shown in Fig. 2. The resulting high temperatures can lead to a feasible application in electric power generation through solar-Rankine power cycles.

The function of the unique tracking mechanism adopted in this concentrator is to maintain the focal line at the working medium tubes independent of the Sun's incidence angle as indicated in Fig. 3. A simple drive system consisting of a fractional horsepower electric motor, reduction gear and an eccentric disk moves the lens assembly on its rollers in a translational motion with simple harmonic motion at a frequency of one cycle per day. Compensation for differences between summer and winter solstice and intermediate seasonal variations is achieved by eccentricity adjustments of the disk.

An important feature of the design is the absence of environmental impact. If water is chosen as the liquid filler for the lenses, it represents little or no hazard in case of leakage failure.

III. Thermal Analysis

This is performed by applying the first law of thermodynamics and the heat rate equations at steady-state condition to the unit concentrator shown in Fig. 2, which is composed of one 2-dimensional lens, a single tube at the lens focal line and the working fluid. After manipulating the energy balance equations for the lens, the tube, and the working fluid, the fluid temperature difference between the inlet and the outlet sections can be written as

$$(T_{out} - T_{in})_1 = [\alpha \tau_1 IR - U_{e1}(T_{in} - T_a)] \frac{1}{U_{e1}} \left[1 - \exp\left(\frac{-U_{e1}U_{pf1}}{RG_f c_f (U_{e1} + U_{pf1})}\right)\right] \quad (1)$$

where U_{pf1} is the tube surface-to-fluid conductance coefficient expressed by Whillier (Ref. 1) for laminar water flow in tubes in the form

$$U_{pf1} = \frac{2.484}{d_i} + \left| \frac{0.0854\left(\frac{m_f}{Ld_i}\right)}{1 + 0.0684\left(\frac{m_f}{L}\right)^{2/3}} \right| \quad (2)$$

The concentrator thermal efficiency is then given by

$$\eta_{th1} = \frac{G_f c_f (T_{out} - T_{in})_1}{I} \quad (3)$$

For comparison, the performance of a flat-plate type collector is given, based on analysis by Whillier (Ref. 1). The comparative flat-plate design is shown in Fig. 4 and includes double glazing and a metallic plate integral with the tubes. The tube's dimensions, lateral spacing, and the optical properties of their coating material are taken the same as for the concentrator. The resulting fluid temperature difference can be written as

$$(T_{out} - T_{in})_2 = [\alpha \tau_2 I - U_{e2}(T_{in} - T_a)] \frac{1}{U_{e2}} \left[1 - \exp\left(\frac{-U_{e2}U_{pf2}}{G_f c_f (U_{e2} + U_{pf2})}\right)\right] \quad (4)$$

where U_{pf2} is the "equivalent" conductance coefficient between the fluid and the combined fin and tubes, given by the following relation

$$\frac{1}{U_{pf2}} = \frac{(d_0 + 2\ell)}{\pi d_i U_{pf1}} + \frac{2\ell(1-F)}{U_{e2}(d_0 + 2\ell F)} \quad (5)$$

where F is the fin efficiency determined from

$$F = \frac{\tanh \ell\sqrt{\frac{U_{e2}}{K\delta}}}{\ell\sqrt{\frac{U_{e2}}{K\delta}}} \quad (6)$$

The corresponding thermal efficiency is then expressed as

$$\eta_{th2} = \frac{G_f c_f (T_{out} - T_{in})_2}{I} \quad (7)$$

Table 1 presents the results of a numerical comparison between the concentrator and the double-glazing collector, and is constructed from the following assumed operating conditions:

Solar radiation intensity	I	= 700 kcal/(h·m²)
Ambient air temperature	T_a	= 20°C
Inlet fluid temperature	T_{in}	= 30°C
Tube surface absorptivity	α	= 0.9
Tube surface emissivity	ϵ	= 0.9
Water-lens transmissivity[1]	τ_1	= 0.78
"Effective" transmissivity of double glazing[2]	τ_2	= 0.83
Water specific heat	c_f	= 1 kcal/kg°C
Tube length	L	= 1.2 m
Tube inner diameter	d_i	= 0.007 m
Tube outer diameter	d_o	= 0.010 m
Half width of fin	ℓ	= 0.075 m
Plate thickness	δ	= 0.0015 m
Tube material conductivity	K	= 45 kcal/(h·m°C) (galvanized steel)
Lens/tube area ratio	R	= 16 (actual concentration ratio)
Number of lens/collector panels		15
Heat loss coefficient between tube (or plate) surface and ambient air[3]	U_{e1}	= 7.33 kcal/h·m²°C
	U_{e2}	= 3.42 kcal/h·m²°C

The above operating conditions were abstracted from the experimental results of flat-plate solar collectors to yield a practical evaluation of their comparison. The efficiency results are plotted as shown in Figs. 5 and 6.

[1]Calculated based on a lens average thickness of 3.81 cm, a refraction index of 1.33 and on extinction coefficient of 0.08 cm^{-1}

[2]Based on 0.32 cm thickness for each panel, an extinction coefficient of 0.08 cm^{-1} and a refraction index of 1.526

[3]U_{e1} is based on an average temperature of 120°C and U_{e2} is based on an average temperature of 70°C.

IV. Conclusions

(1) The improved efficiency of the concentrator compared with the double-glazing collector at a given radiation intensity and a wide range of fluid mass flux is plotted in Fig. 5. The percentage improvement in efficiency is also included for comparison in Table 1. It appears that the thermal efficiency obtained from the concentrator exceeds that of the comparative double-glazing collector for all operating conditions. As an example, for a high temperature application where the fluid is heated by 175°C, the corresponding mass flux is 2.5 kg/(h·m²) and an improvement in the thermal efficiency of 76 percent is obtained. On the other hand, for a high efficiency operation, Table 1 indicates that a large mass flux of 100 kg/(h·m²) gives an efficiency improvement of 13 percent over the double-glazing collector, which is still considered a useful gain in collector performance.

(2) The performance curve expressing the thermal efficiency vs. the variable $(T_{in} - T_a)/I$ at a selected mass flux of 30 kg/(h·m²) is as shown in Fig. 6. The straight line relationship is evident from the fluid temperature rise expressions given by Eqs. (1) and (4). For the concentrator, the thermal efficiency can be written as

$$\eta_{th1} = 0.684 - 0.447\left(\frac{T_{in} - T_a}{I}\right) \tag{8}$$

and that for the double-glazing collector as

$$\eta_{th2} = 0.619 - 2.835\left(\frac{T_{in} - T_a}{I}\right) \tag{9}$$

The "zero-efficiency" condition, with a radiation intensity of 700 kcal/(h·m²), corresponds to an inlet fluid temperature of 1072°C for the concentrator and 153°C for the double-glazing collector. This result shows that the maximum temperatures that can be reached by the concentrator are much higher than is possible with the comparative double-glazing type.

(3) The slope of the performance curves of Fig. 6, which is a measure of the heat loss, is shown to have a smaller value for the concentrator compared with the double-glazing collector. This is due to the fact that in the case of the concentrator the heat loss coefficient between the tube and the ambient air per unit area of the collector is given

by U_{e1}/R, while that for the double-glazing type is U_{e2}. This means that the reduction in heat losses to the surroundings, brought by focusing the incident energy on a smaller area, outweighs its increase due to higher temperatures obtained.

(4) Practical examples of the utilization of the present concentrator in airconditioning and/or power generation applications, are taken from Table 1 as follows:

(a) For an electric-power generation application, a mass flux of 2.5 kg/(h·m²) is chosen for each concentrator panel (1.2 × 2.4 m) which results in an exit fluid temperature of 204.7°C. If a Rankine power cycle is operated between 204.7°C and an ambient temperature 20°C as its temperature limits at 50 percent relative efficiency to the Carnot cycle, it will give a thermal efficiency of 19 percent. This means that one concentrator panel can produce a mechanical work equivalent to 0.28 kW per panel for every hour of operation.

(b) It appears feasible for the airconditioning load of a normal residence (3 tons of refrigeration) to be carried out totally by solar energy. For example, if the airconditioner used is a mechanical vapor compression refrigeration unit that is driven by a solar-Rankine cycle it will consume about 3.6 kW. In this case, 12.8 concentrator panels are needed with a total area of 37 m² (400 ft²).

On the other hand, if the airconditioner used is of the absorption type, a collector temperature in the order of 100°C is sufficient. A mass flux of 5 kg/(h·m²) from Table 1 will result in a fluid temperature of 121.3°C, which is adequate for full-load operation (coefficient of performance is about 0.65). In this case, only 10.6 concentrator panels are needed for airconditioning the house with a total area of 30.6 m² (328 ft²). Both cases indicate that the required collection area for airconditioning is adequate and does not exceed that of a south-facing roof in most houses.

Definition of terms

c_f	fluid specific heat, kcal/kg·°C
d_i	inner tube diameter, m
d_o	outer tube diameter, m
F	fin efficiency
G_f	fluid mass flux (flow rate per unit collector area), kg/h·m²
I	solar radiation intensity, kcal/(h·m²)
K	conductivity, kcal/(h·m°C)
ℓ	half width of fin, m
L	tube length, m
m_f	mass flow rate per tube, kg/hr
R	lens area/concentrator tube projected area
T_{in}	inlet fluid temperature, °C
T_{out}	outlet fluid temperature, °C
T_a	ambient temperature, °C
U_e	"effective" heat loss coefficient between tube (or plate) surface and ambient, kcal/(hr·m²·°C)
U_{pf}	tube (or plate) surface to fluid conductance coefficient, kcal/h·m²·°C)
α	absorptivity
τ	transmissivity
δ	plate thickness, m
ϵ	emissivity
η_{th}	thermal efficiency

Subscripts

1	concentrator
2	double-glazing collector

Reference

1. Whillier, A., "Design Factors Influencing Solar Collector Performance," *Low Temperature Engineering Application of Solar Energy*, ASHRAE Publication, 1967, Chap. III, pp. 27–40.

Table 1. Numeric comparison between solar concentrator and analogous flat-plate double-glazing collector

G_f, kg/(h•m²)	Flow rate per tube, kg/h	Fluid temperature rise, $(T_{out}-T_{in})$ °C		Thermal efficiency η, %		% Improvement in efficiency
		Concentrator	Double-glazing	Concentrator	Double-glazing	
0	0	1062.6	142.9	00.0	00.0	0
2.5	0.48	174.7	99.1	62.4	35.4	76
5	0.96	91.3	63.8	65.2	45.6	43
10	1.92	46.7	36.6	66.7	52.4	27
20	3.84	23.6	19.7	67.5	56.4	20
30	5.76	15.8	13.5	67.8	57.9	17
50	9.6	9.5	8.3	68.1	59.2	15
100	19.2	4.8	4.2	68.4	60.5	13

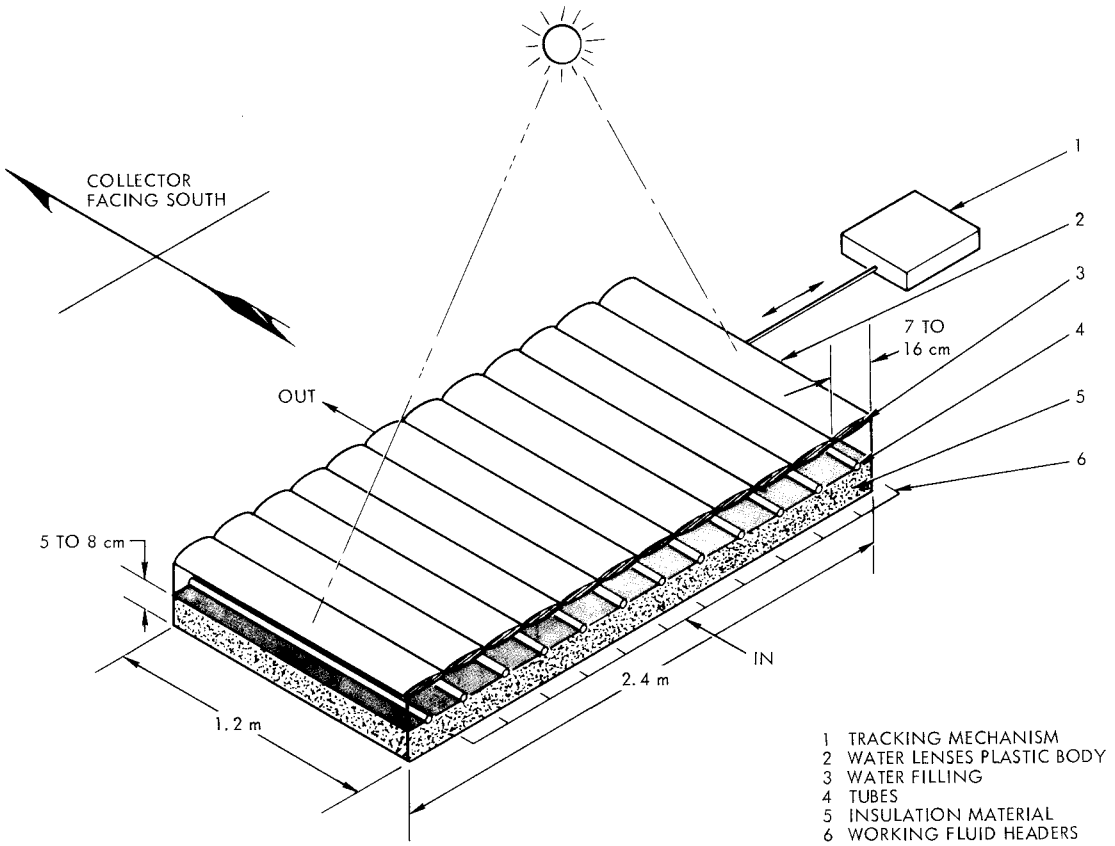

Fig. 1. Overall view of the solar concentrator

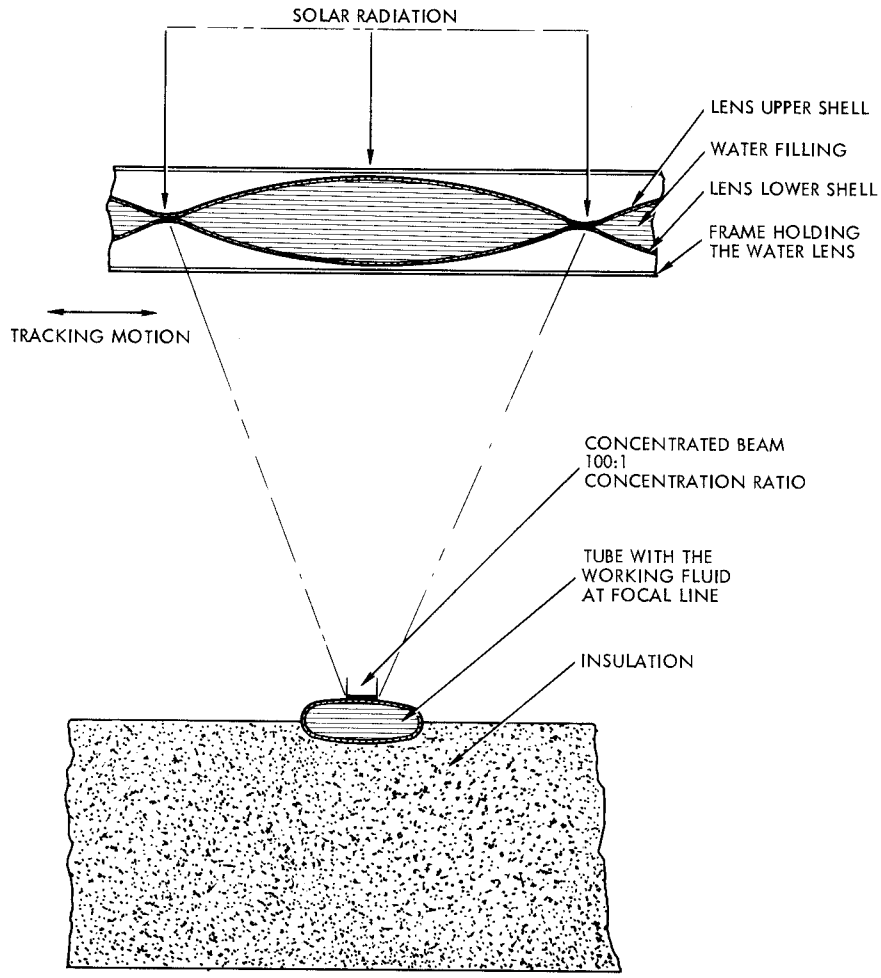

Fig. 2. Working principle of a "liquid" lens

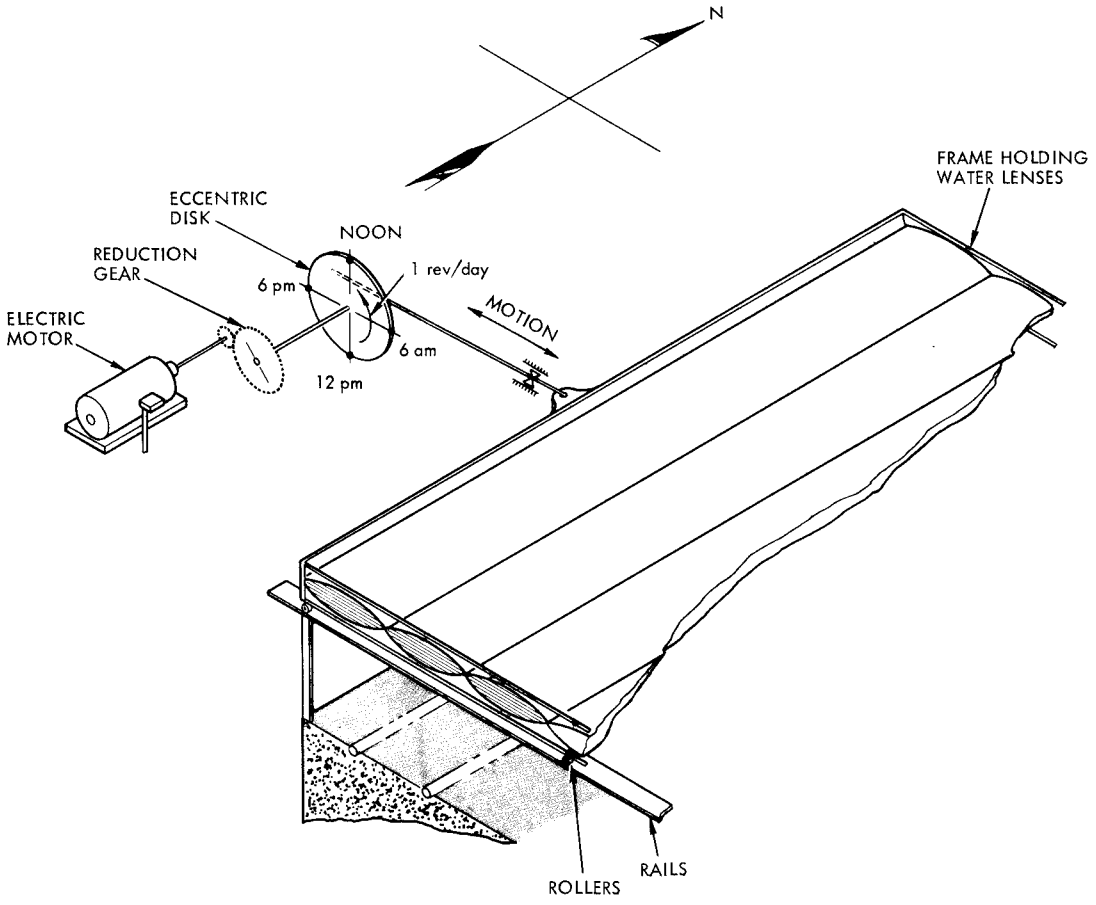

Fig. 3. Details of translational tracking mechanism

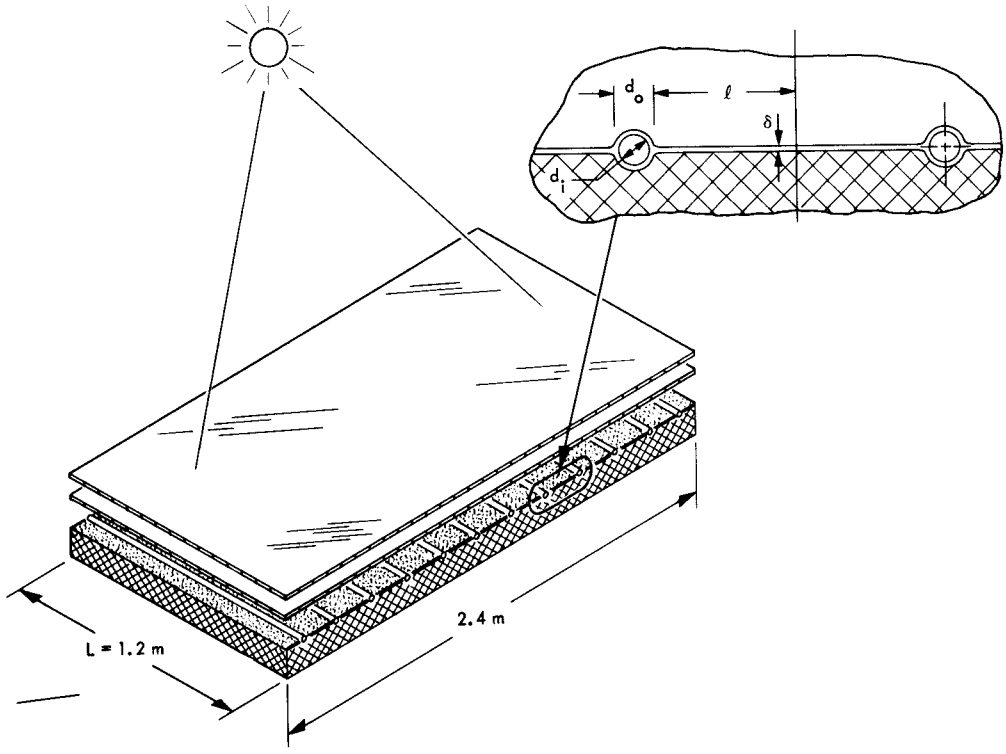

Fig. 4. Double-glazing flat-plate solar collector

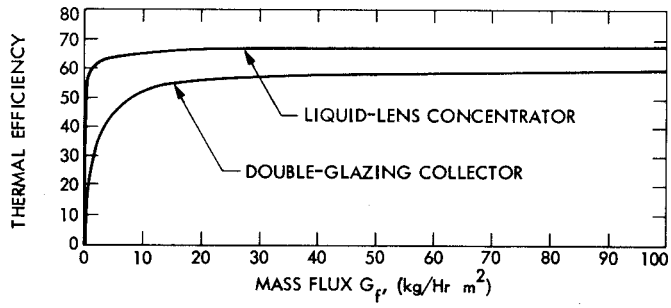

Fig. 5. Effect of varying the mass flux on the collector thermal efficiency

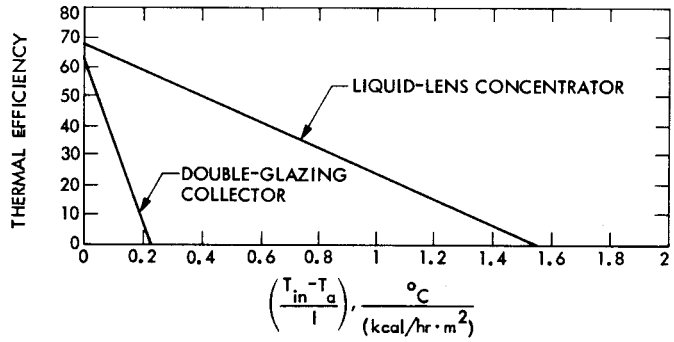

Fig. 6. Efficiency curves for a flow flux G_f = 30 kg/h · m²